1-1-2011

Asymptotic and numerical results for a model of solvent-dependent drug diffusion through polymeric spheres

Scott McCue
Queensland University Of Technology, scott.mccue@qut.edu.au

Mike Hsieh
Queensland University Of Technology

Timothy J. Moroney
Queensland University Of Technology, t.moroney@qut.edu.au

Mark I. Nelson
University of Wollongong, mnelson@uow.edu.au

Asymptotic and numerical results for a model of solvent-dependent drug diffusion through polymeric spheres

Abstract

A model for drug diffusion from a spherical polymeric drug delivery device is considered. The model contains two key features. The first is that solvent diffuses into the polymer, which then transitions from a glassy to a rubbery state. The interface between the two states of polymer is modeled as a moving boundary, whose speed is governed by a kinetic law; the same moving boundary problem arises in the one-phase limit of a Stefan problem with kinetic undercooling. The second feature is that drug diffuses only through the rubbery region, with a nonlinear diffusion coefficient that depends on the concentration of solvent. We analyze the model using both formal asymptotics and numerical computation, the latter by applying a front-fixing scheme with a finite volume method. Previous results are extended and comparisons are made with linear models that work well under certain parameter regimes. Finally, a model for a multilayered drug delivery device is suggested, which allows for more flexible control of drug release.

Keywords

polymeric, diffusion, asymptotic, numerical, drug, spheres, dependent, solvent, model, results

Disciplines

Physical Sciences and Mathematics

Publication Details

McCue, S., Hsieh, M., Moroney, T. J. & Nelson, M. I. (2011). Asymptotic and numerical results for a model of solvent-dependent drug diffusion through polymeric spheres. SIAM Journal on Applied Mathematics, 71 (6), 2287-2311.

SIAM J. APPL. MATH.
Vol. 71, No. 6, pp. 2287–2311

ASYMPTOTIC AND NUMERICAL RESULTS FOR A MODEL OF SOLVENT-DEPENDENT DRUG DIFFUSION THROUGH POLYMERIC SPHERES*

SCOTT W. MCCUE†, MIKE HSIEH†, TIMOTHY J. MORONEY†, AND MARK I. NELSON‡

Abstract. A model for drug diffusion from a spherical polymeric drug delivery device is considered. The model contains two key features. The first is that solvent diffuses into the polymer, which then transitions from a glassy to a rubbery state. The interface between the two states of polymer is modeled as a moving boundary, whose speed is governed by a kinetic law; the same moving boundary problem arises in the one-phase limit of a Stefan problem with kinetic undercooling. The second feature is that drug diffuses only through the rubbery region, with a nonlinear diffusion coefficient that depends on the concentration of solvent. We analyze the model using both formal asymptotics and numerical computation, the latter by applying a front-fixing scheme with a finite volume method. Previous results are extended and comparisons are made with linear models that work well under certain parameter regimes. Finally, a model for a multilayered drug delivery device is suggested, which allows for more flexible control of drug release.

Key words. controlled drug release, solvent penetration, glassy-rubbery polymer transition, moving boundary problem, multilayer system, formal asymptotics, kinetic undercooling

AMS subject classifications. 35R37, 74N25, 80A22

DOI. 10.1137/110821688

1. Introduction.

The role of solvent diffusion in polymer systems is critically important for a variety of drug delivery processes. In terms of mathematical modeling, there are numerous studies of interest, many of which involve linear diffusion on fixed domains, allowing for exact solutions and relatively simple formulae for drug release and other important variables [11]. In the context of drug delivery, detailed reviews of such models for solvent penetration in polymers include [5], for example.

In the present study, we are interested in polymers (such as hydroxypropyl methylcellulose) that are initially in a dry glassy state before being immersed in a body of thermodynamically compatible solvent. Provided the concentration of solvent U is above a certain threshold value U^*, the solvent diffuses into the polymer, significantly weakening the entanglement of macromolecular polymer chains, and transforming the affected region of polymer to a rubbery or gel-like phase. The narrow layer dividing the glassy and rubbery regions can be thought of as a moving interface which penetrates into the polymer. At the same time, the intake of solvent causes the rubbery region to swell, while the dissolved polymer chains on the polymer/solvent interface diffuse away into the solvent. Of course the extent of solvent penetration, polymer swelling, and polymer dissolution depends on the properties of the polymer and solvent in question.

There exists a number of mathematical models for the above processes, including the early studies [2, 21, 39, 26, 51, 52] and good reviews by [37, 38]. Here we are interested in those mathematical models for which the glassy-rubbery inter-

*Received by the editors January 20, 2011; accepted for publication (in revised form) August 8, 2011; published electronically December 20, 2011.
http://www.siam.org/journals/siap/71-6/82168.html
†School of Mathematical Sciences, Queensland University of Technology, Brisbane QLD 4001, Australia (scott.mccue@qut.edu.au, m2.hsieh@student.qut.edu.au, t.moroney@qut.edu.au).
‡School of Mathematics and Applied Statistics, University of Wollongong, Wollongong NSW 2522, Australia (mnelson@uow.edu.au).

face is described by a moving boundary whose kinetics is governed by an empirical law that relates the concentration of solvent there to the velocity of the interface. In particular, we revisit the model studied in Astarita and Sarti [6] and others [3, 9, 13, 14, 15, 16, 18, 19, 20, 28, 29], which has the appealing feature that the moving boundary evolves with constant speed in the small time limit, in line with known experimental data [2, 6, 36]. In section 2 we formulate the model for a spherical polymeric particle (as in Lin et al. [29]), so that the glassy-rubbery interface moves toward the center of the sphere. By applying formal asymptotics in section 2.3, we are able to determine a number of terms in the small-time expansion and observe the transition to a completely different qualitative behavior (which has the interface initially moving with infinite speed) as the important kinetic parameter vanishes, the implication being that models that do not apply the kinetic law on the glassy-rubbery interface (such as [26, 39, 41, 51, 52], for example) cannot recover the appropriate small-time behavior. The moving boundary problem is solved numerically using a front-fixing transformation together with a finite volume spatial discretization (section 2.4). We also provide an asymptotic analysis of the moving boundary in the limit that the control parameter is large (section 2.5), as well as numerical results for the limit that the glassy-rubbery interface reaches the center of the sphere (section 2.6). At this point it is worth mentioning that some authors use the term "free boundary" instead of "moving boundary"; following the convention of Crank [12], we use the latter, as the governing equations are parabolic.

We note that the model treated in section 2 also applies for a one-phase Stefan problem with kinetic undercooling (a careful derivation of this one-phase model from a two-phase formulation is presented in [15]). For the geometry considered here, the Stefan problem describes the melting of an ice-ball initially at its melting temperature. In that context, the asymptotic limits considered in this paper are early melting, large Stefan number, and near-complete-melting. In particular, we extend the large Stefan number analysis presented in Riley, Smith, and Poots [48], Soward [49], and Stewartson and Waechter [50] to hold for nonzero kinetic undercooling (in the same way as [53] generalizes the classical problem to include surface tension). Further, we observe that the inclusion of kinetic undercooling regularizes a singularity in the near-complete-melting limit.

There are a plethora of mathematical models that describe drug diffusion processes, many of which essentially involve linear diffusion in a fixed domain [11]. We are interested in studying drug release from polymers in contact with solvent, which leads to more sophisticated modeling, since the drug mobility is much higher in the rubbery region of polymer, and the width of the rubbery region changes as the glassy-rubbery interface propagates into the polymer and the rubbery polymer swells or even dissolves into the surrounding solvent. The most notable and/or highly cited mathematical models are presented by Peppas and coworkers [8, 40, 43, 44, 46], with more general reviews of models that couple the processes of drug release, solvent diffusion, and the glassy-rubbery transition given in [5, 27, 45, 47].

In section 3, we are concerned with a model for drug release from a spherical polymer device that is an extension of that treated in Cohen and Erneux [10], who coupled drug diffusion with the one-dimensional moving boundary problem for solvent penetration [6, 9] described above. The first extension is to apply the model to a spherical geometry, as was also done by Lin and Peng [30]. In addition, we use a nonlinear diffusion coefficient that depends on the concentration of solvent, further coupling the processes. The model itself is described in section 3.1, and then asymptotic limits of small time and large control parameter are treated briefly in section 3.2,

where we show how the kinetic parameter mentioned above is crucial in determining qualitative behavior. In section 3.3 we present numerical results that suggest that for some parameter regimes a simple linear diffusion model works essentially as well as the more complicated coupled moving boundary problem. Finally, we extend the model further to apply in a multilayered device in section 3.4, allowing for greater control of drug release from the polymer.

We finish the paper in section 4 with a short discussion of the results and how the models can be extended to include the effects of polymer swelling.

2. Model for diffusion of solvent into polymeric spheres.

2.1. Mathematical formulation. We suppose that initially a spherical ball of glassy polymer is immersed in a solvent which subsequently diffuses into the polymer. We denote the concentration of solvent in the polymer by $U(R,T)$, where R is the radial coordinate and T is time. As the solvent penetrates the polymer, an interface $R = S(T)$ divides the inner glassy region $0 < R < S(T)$ from the rubbery region $S(T) < R < S(0)$, where $S(0)$ is the radius of the ball (at $T = 0$ there is no rubbery region).

The moving boundary problem for U with which we shall be concerned is

$$\text{in} \quad S(T) < R < S(0), \qquad \frac{\partial U}{\partial T} = D\frac{1}{R^2}\frac{\partial}{\partial R}\left(R^2\frac{\partial U}{\partial R}\right), \tag{2.1}$$

$$\text{on} \quad R = S(0), \qquad U = U_0, \tag{2.2}$$

$$\text{on} \quad R = S(T), \qquad D\frac{\partial U}{\partial R} = -(U+K)\frac{\mathrm{d}S}{\mathrm{d}T}, \tag{2.3}$$

$$\text{on} \quad R = S(T), \qquad k(U-U^*)^n = -\frac{\mathrm{d}S}{\mathrm{d}T}, \tag{2.4}$$

where $U_0 > U^*$. Equation (2.1) describes diffusion of solvent in the rubbery region $S(T) < R < S(0)$ with a constant diffusivity D, while (2.2) forces the concentration of solvent to be the constant U_0 on the outside of the ball. The remaining two equations are conditions on the moving boundary $R = S(T)$: (2.3) is a mass balance, while (2.4) describes a kinetic law that states that there is a threshold value U^* above which the interface will move with a speed given by a power law with index $n > 0$. The problem (2.1)–(2.4) is treated in [29], while the one-dimensional version has received much more attention [6, 9, 13, 14, 15, 16, 28] (we refer the reader to these studies for more details of the formulation). While the governing equation (2.1) is linear, the entire problem (2.1)–(2.4) is nonlinear due to the moving boundary.

We scale (2.1)–(2.4), introducing the dimensionless variables

$$r = \frac{R}{S(0)}, \quad t = \frac{DT}{S(0)^2}, \quad u(r,t) = \frac{U-U^*}{U_0-U^*}, \quad s(t) = \frac{S(T)}{S(0)} \tag{2.5}$$

to give

$$\text{in} \quad s(t) < r < 1, \qquad \frac{\partial u}{\partial t} = \frac{1}{r^2}\frac{\partial}{\partial r}\left(r^2 \frac{\partial u}{\partial r}\right), \tag{2.6}$$

$$\text{on} \quad r = 1, \qquad u = 1, \tag{2.7}$$

$$\text{on} \quad r = s(t), \qquad \frac{\partial u}{\partial r} = -(u+\lambda)\frac{\mathrm{d}s}{\mathrm{d}t}, \tag{2.8}$$

$$\text{on} \quad r = s(t), \qquad u^n = -\mu \frac{\mathrm{d}s}{\mathrm{d}t}, \tag{2.9}$$

$$\text{at} \quad t = 0, \qquad s = 1, \tag{2.10}$$

where, in addition to the index n, the two dimensionless parameters in the problem are

$$\mu = \frac{D}{kS(0)(U_0 - U^*)^n}, \quad \lambda = \frac{U^* + K}{U_0 - U^*}. \tag{2.11}$$

Typically, the kinetic parameter μ is small, while the control parameter λ can range from $\mathcal{O}(1)$ to large [7, 24, 39, 46]. It is quite common to take the kinetic law (2.9) to be a simple linear relationship, with $n = 1$. For most of the study we use this value. We emphasize that there are no known exact solutions to (2.6)–(2.10), even for the case $\mu = 0$ (unlike in the one-dimensional counterpart, which has the well-known Neumann solution for $\mu = 0$ [11, 12]).

In the well-studied one-dimensional counterpart to (2.6)–(2.10), the moving boundary propagates for all time, whereas in the spherical case we are considering here, the interface will eventually reach the center $r = 0$, at which time the entire polymer ball will be in the rubbery state. We call this the extinction time t_{e} and consider the limit $t \to t_{\mathrm{e}}^-$ in section 2.6. For now we note that for $t > t_{\mathrm{e}}$, the diffusion process can continue, governed by the linear problem (2.6) (with the domain changed to $0 < r < 1$), (2.7), and the condition

$$\text{on} \quad r = 0, \quad \frac{\partial u}{\partial r} = 0. \tag{2.12}$$

As is well known, the solution to this linear problem has $u(r,t) \to 1$ as $t \to \infty$ for all r.

2.2. Stefan problem with kinetic undercooling. At this stage it is worth describing how (2.6)–(2.10) arises in the context of melting an ice-ball. Consider a solid ball of ice, initially at melting temperature U^*, which has its surface temperature suddenly raised to $U_0 > U^*$. Under idealized conditions (ignoring the effects of gravity, for example), the ball will begin to melt with an interface $R = S(T)$ between the solid and liquid regions propagating toward the center of the ball. If we now use $U(R,T)$ to denote temperature in the liquid region $S(T) < R < S(0)$, the governing equation is (2.1), where now D is the thermal diffusivity. The condition (2.2) still holds, but (2.3) and (2.4) are replaced by

$$\text{on} \quad R = S(T), \qquad D\frac{\partial U}{\partial R} = -\frac{L}{c_{\mathrm{p}}}\frac{\mathrm{d}S}{\mathrm{d}T}, \tag{2.13}$$

$$\text{on} \quad R = S(T), \qquad U = U^*, \tag{2.14}$$

where L is the latent heat of fusion per unit mass, while c_{p} is the specific heat of the liquid at constant pressure. Applying the scalings (2.5), the dimensionless one-phase

problem for melting an ice-ball becomes (2.6)–(2.10) with $\mu = 0$, where now λ is the Stefan number $\lambda = L/c_{\rm p}(U_0 - U^*)$. In this context the extinction time $t_{\rm e}$ is the time it takes for complete melting of the ice-ball.

If we now take into account the (normally weak) effect of kinetic undercooling on the solid-melt interface, then instead of (2.14) we again have (2.4), where now k is the kinetic undercooling parameter. However, we cannot simply keep (2.13), as this condition holds only if there is no flux of heat within the inner solid phase (as in the case in which kinetic undercooling is ignored, for which temperature in the solid phase is identically equal to the melting temperature U^* for all time). Instead, the full two-phase problem must be treated, from which the physically meaningful condition

$$\text{on} \quad R = S(T), \qquad D\frac{\partial U}{\partial R} = -\left(\frac{L}{c_{\rm p}} + U - U^*\right)\frac{{\rm d}S}{{\rm d}T} \tag{2.15}$$

appears to leading order in the limit that the thermal diffusivity in the solid vanishes. The scalings (2.5) now lead to (2.6)–(2.10), where λ is the Stefan number, and μ is the dimensionless kinetic undercooling parameter. Full details of the derivation of (2.15) are included in [15, 25].

2.3. Asymptotic limit $t \to 0^+$. We determine the small-time behavior using the front-fixing transformation

$$\xi = \frac{r - s}{1 - s}, \tag{2.16}$$

which has the property that $r = s$ corresponds to $\xi = 0$ and $r = 1$ corresponds to $\xi = 1$. By applying the ansatz

$$u \sim \frac{1}{r}\left\{u_0(\xi) + u_1(\xi)(1-s) + u_2(\xi)(1-s)^2\right\}, \tag{2.17}$$

$$t \sim a_1(1-s) + a_2(1-s)^2 + a_3(1-s)^3 \tag{2.18}$$

we are able to solve for the u_i and

$$a_1 = \mu, \quad a_2 = \frac{n}{2}(1+\lambda), \quad a_3 = -\frac{n}{6\mu}\left[(n-1)\lambda^2 + 2(n+\mu)\lambda + 1 + n + 2\mu\right], \tag{2.19}$$

resulting in the asymptotic behavior

$$u \sim 1 - \frac{1+\lambda}{\mu}\left(\frac{1-r}{r}\right) + \frac{(1+\lambda)(1+2\mu+n(1+\lambda))}{\mu^3}\left(\frac{1-r}{r}\right)t, \tag{2.20}$$

$$s \sim 1 - \frac{1}{\mu}t + \frac{n(1+\lambda)}{2\mu^3}t^2 - \frac{n[(4n-1)\lambda^2 + (8n+2\mu)\lambda + 1 + 4n + 2\mu]}{6\mu^5}t^3 \tag{2.21}$$

as $t \to 0^+$.

While the results (2.20)–(2.21) have not been presented previously, they are perfectly analogous to the small-time expansions for the one-dimensional problem recorded in [6, 9, 14, 15, 16]; using x as the Cartesian coordinate for the one-dimensional problem, these are

$$u \sim 1 - \frac{1+\lambda}{\mu}(1-x) + \frac{(1+\lambda)(1+n(1+\lambda))}{\mu^3}(1-x)t, \tag{2.22}$$

$$s \sim 1 - \frac{1}{\mu}t + \frac{n(1+\lambda)}{2\mu^3}t^2 - \frac{n[(4n-1)\lambda^2 + 8n\lambda + 1 + 4n]}{6\mu^5}t^3 \tag{2.23}$$

as $t \to 0^+$. We see that (2.20)–(2.21) differ from (2.22)–(2.23) only in the higher order terms, which is as expected, since for small time the domain $s(t) < r < 1$ is a thin shell that is almost one-dimensional.

The main point of interest regarding (2.20)–(2.21) is that $1 - s = \mathcal{O}(t)$ as $t \to 0^+$, meaning that speed of the interface is finite at $t = 0^+$ (this phenomenon, which is associated with $\partial u/\partial r(1,t) = \mathcal{O}(1)$ as $t \to 0^+$, is often confusingly referred to as "non-Fickian" or Case II diffusion, even though the diffusion itself is governed by Fick's law), whereas in the well-studied case $\mu = 0$ (corresponding to the classical one-phase Stefan problem) we have $1 - s = \mathcal{O}(t^{1/2})$ in the limit, corresponding to an interface speed that has the (unphysical) behavior $\mathrm{d}s/\mathrm{d}t \to -\infty$ as $t \to 0^+$. Thus the addition of kinetic undercooling has the effect of regularizing the classical one-phase Stefan problem in the small time limit. But more importantly in the present context, a consequence of having a finite interface speed as $t \to 0^+$ (Case II diffusion) is that, when coupled with our model for drug diffusion, we find that the drug is released at a constant rate initially (that is, the outward flux of the drug on the boundary of the sphere is finite in the limit $t \to 0^+$; see (3.12)–(3.13) and the subsequent paragraph), which is a desirable outcome from a pharmaceutical perspective. We defer this discussion until section 3.2 but note that models for solvent penetration that do not include a kinetic law on the interface are deficient in this respect.

To reconcile the different small-time scalings for $\mu > 0$ and $\mu = 0$, we note that for $\mu \ll 1$, (2.20)–(2.21) are valid for $t = \mathcal{O}(\mu^2)$ and $1 - s = \mathcal{O}(\mu)$, but these expansions break down for $\mu^2 \ll t \ll 1$ and $\mu \ll 1 - s \ll 1$, reflecting the fact that the limits $t \to 0^+$ and $\mu \to 0^+$ do not commute. By posing $1 - r = \mu^\gamma \tilde{r}$, $t = \mu^{2\gamma}\tilde{t}$, and $1 - s = \mu^\gamma \tilde{s}$, where γ is a constant and $\tilde{r} = \mathcal{O}(1)$, $\tilde{t} = \mathcal{O}(1)$, $\tilde{s} = \mathcal{O}(1)$, we can write $u \sim \tilde{u}_0(\tilde{r}, \tilde{t})$, $\tilde{s} \sim \tilde{s}_0$ as $\mu \to 0^+$, so that (2.6)–(2.8), (2.10) become

$$\text{in} \quad 0 < \tilde{r} < \tilde{s}_0(\tilde{t}), \qquad \frac{\partial \tilde{u}_0}{\partial \tilde{t}} = \frac{\partial^2 u}{\partial \tilde{r}^2}, \tag{2.24}$$

$$\text{on} \quad \tilde{r} = 0, \qquad \tilde{u}_0 = 1, \tag{2.25}$$

$$\text{on} \quad \tilde{r} = \tilde{s}_0(\tilde{t}), \qquad \frac{\partial \tilde{u}_0}{\partial \tilde{r}} = -(\tilde{u}_0 + \lambda)\frac{\mathrm{d}\tilde{s}_0}{\mathrm{d}\tilde{t}}, \tag{2.26}$$

$$\text{at} \quad \tilde{t} = 0, \qquad \tilde{s}_0 = 0. \tag{2.27}$$

Now, to leading order, the left-hand side of (2.9) is $\tilde{u}_0^n$, while the right-hand side is $\mu^{1-\gamma}\mathrm{d}\tilde{s}_0/\mathrm{d}\tilde{t}$, so we have

$$\text{on} \quad \tilde{r} = \tilde{s}_0(\tilde{t}), \qquad \begin{cases} \tilde{u}_0 = 0, & \gamma < 1, \\ \tilde{u}_0^n = \dfrac{\mathrm{d}\tilde{s}_0}{\mathrm{d}\tilde{t}}, & \gamma = 1. \end{cases} \tag{2.28}$$

Thus $\gamma = 1$ is seen to be the critical exponent, with $\gamma \geq 1$ corresponding to the small-time behavior (2.20)–(2.21). On the other hand, the case $\gamma < 1$ has the small-time asymptotics governed by (2.24)–(2.27), $(2.28)_1$, which is of course the classical one-phase Stefan problem in one dimension, with the exact solution (the Neumann solution)

$$\tilde{u}_0 = 1 - \frac{\operatorname{erf}(\tilde{r}/2\tilde{t}^{1/2})}{\operatorname{erf}(\alpha)}, \quad \tilde{s}_0 = 2\alpha\tilde{t}^{1/2},$$

where α is the positive real root of the transcendental equation

$$\sqrt{\pi}\alpha\lambda \mathrm{e}^{\alpha^2}\operatorname{erf}(\alpha) = 1 \tag{2.29}$$

(see [11, 12]).

2.4. Numerical scheme. To solve (2.6)–(2.10) numerically we first transform the problem to a fixed domain by applying the front-fixing transformation (2.16) and then taking the approach of [31] to cast the transport equation in conservative form. The resulting problem

$$\text{in} \quad 0 < \xi < 1, \qquad \frac{\partial}{\partial t}\left\{u(1-s)[s+(1-s)\xi]^2\right\}$$

$$= \frac{\partial}{\partial \xi}\left\{\frac{[s+(1-s)\xi]^2}{1-s}\left[\frac{\partial u}{\partial \xi} + u(1-\xi)(1-s)\frac{\mathrm{d}s}{\mathrm{d}t}\right]\right\}, \tag{2.30}$$

$$\text{on} \quad \xi = 1, \qquad u = 1, \tag{2.31}$$

$$\text{on} \quad \xi = 0, \qquad \frac{\partial u}{\partial \xi} = \frac{(u+\lambda)(1-s)u^n}{\mu}, \tag{2.32}$$

$$\text{on} \quad \xi = 0, \qquad \frac{\mathrm{d}s}{\mathrm{d}t} = -\frac{u^n}{\mu} \tag{2.33}$$

is then amenable to a numerical discretization on the fixed interval $0 \le \xi \le 1$. We introduce $N-1$ internal mesh nodes in order to subdivide the interval into N subintervals and apply a finite volume spatial discretization of (2.30). The boundary conditions at $\xi = 0$ and $\xi = 1$ are provided by (2.32) and (2.31), respectively. For the sensitive computations presented below in subsection 2.6, the behavior of which we are interested in as $s \to 0^+$ (or $t \to t_{\mathrm{e}}^-$), we use a nonuniform mesh, with the smallest subinterval beginning at $\xi = 0$, and subinterval widths growing geometrically away from this point.

The resulting semidiscrete problem is a system of N ordinary differential equations in time, with one equation for the scaled concentration at each internal node, and at the boundary node $\xi = 0$ (the Dirichlet condition imposed at $\xi = 1$ provides the solution there). This system is coupled with the additional equation (2.33), which describes the motion of the moving boundary, to give a system of $N+1$ ordinary differential equations.

This method-of-lines formulation allows a standard initial value problem solver to be used to advance the solution in time. We use MATLAB's `ode15s`, which employs variable-order, variable-stepsize numerical differentiation formulae [42]. The small-time expansions (2.20) and (2.21) are used to construct initial conditions for the problem at a time shortly after $t = 0$. We note that for performance reasons it is imperative that the sparsity pattern of the Jacobian matrix be specified in the call to `ode15s`. Using a mesh of $N = 10,000$ nodes, the code requires around ten minutes to solve on a standard desktop machine.

A typical numerical solution is illustrated in Figure 2.1, computed using the representative parameter values $\lambda = 1$, $\mu = 0.1$. Part (a) shows profiles of solvent concentration u versus radius r for different times. For these parameter values, the extinction time is roughly $t_{\mathrm{e}} = 0.4$, at which point the glassy-rubbery interface reaches the center of the sphere. The evolution of the interface $r = s(t)$ versus time is shown in part (b).

We note that Lin et al. [29] also solve (2.6)–(2.10) numerically, except they use a different approach, which they call a local similarity method, which involves approximating the solution on each time interval with a self-similar form appropriate for the one-dimensional problem with $\mu = 0$. From the results presented in their paper, which do not include any profiles of solvent concentration, it is not clear from their study how well their scheme works. This is especially true in the delicate limit $t \to t_{\mathrm{e}}^-$, given that their approximation on each time step becomes less valid as time

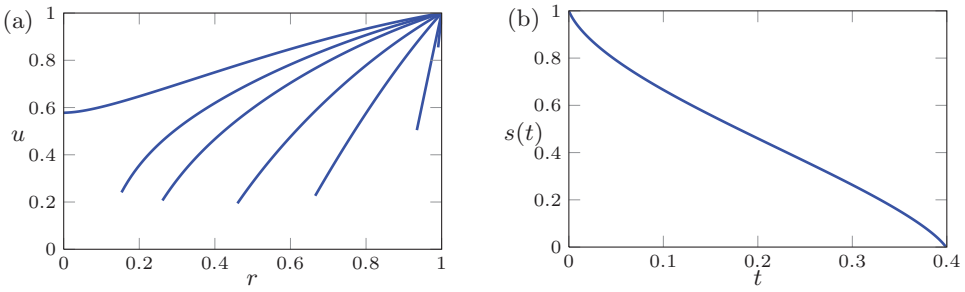

FIG. 2.1. *Numerical solution of* (2.6)–(2.10) *computed for* $\lambda = 1$ *and* $\mu = 0.1$. (a) *From right to left, profiles of solvent concentration* u *versus radius* r *are shown for times* $t = 0.001$, 0.01, 0.1, 0.2, 0.3, 0.35, *and* 0.3991. (b) *Dependence of glassy-rubbery interface* $r = s(t)$ *on time* t.

increases. Despite this possible inaccuracy, the reader is referred to [29] for some typical numerical results, including the effect that varying n has on the location and speed of the glassy-rubbery interface.

2.5. Asymptotic limit $\lambda \to \infty$. In this subsection we treat (2.6)–(2.10) for $\lambda \gg 1$. For this regime the glassy-rubbery interface moves relatively slowly, with the extinction time (the time it takes for the interface to reach the center) $t_e = \mathcal{O}(\lambda)$ (remember that the problem has been scaled so that solvent diffuses a distance $\mathcal{O}(1)$ over a time period $\mathcal{O}(1)$). For the special case $\mu = 0$ this difficult problem has three time scales: $t = \mathcal{O}(\lambda)$, $t_e - t = \mathcal{O}(1)$, and $t_e - t = \mathcal{O}(\exp(-2\sqrt{2\pi}\lambda^{1/2}))$. The first two time scales are dealt with in [48], for example, while the final exponentially short time scale is resolved in [49, 50] (the two-phase problem with $\mu = 0$ is studied in [34], and the analysis for arbitrary two- and three-dimensional domains is provided in [32, 33]).

For $\mu > 0$ we must consider an earlier time scale $t = \mathcal{O}(\mu^2/\lambda)$, as the subsequent time scale $t = \mathcal{O}(\lambda)$ does not resolve the small-time behavior described in subsection 2.3. A similar undertaking was attempted in Lin et al. [29], except these authors treat only the leading order term. For the case $n = 1$ we give two correction terms and go on to provide a rather complete analysis for next two time scales.

2.5.1. Time scale 1, $t = \mathcal{O}(\mu^2/\lambda)$, $1 - s = \mathcal{O}(\mu/\lambda)$. For this short time scale we work with the variables

$$\rho = \frac{\lambda}{\mu} r, \quad \tau = \frac{\lambda}{\mu^2} t, \quad \sigma(\tau) = \frac{\lambda}{\mu} s(t), \tag{2.34}$$

so that the outer radius of the sphere ($r = 1$) is given by

$$\rho_f = \frac{\lambda}{\mu}. \tag{2.35}$$

As a result, the parameter μ is scaled out of the governing equations (2.6)–(2.10), leading to dimensionless variables that are employed in Lin et al. [29] (who do not take the radius of the sphere to be a representative length scale).

To proceed, we swap the roles of τ and σ and consider τ to be a function of σ, which we treat as an independent variable. Expanding u and τ in the form

$$u \sim u_0(\rho, \sigma) + \frac{u_1(\rho, \sigma)}{\lambda} + \frac{u_2(\rho, \sigma)}{\lambda^2}, \quad \tau \sim \tau_0(\sigma) + \frac{\tau_1(\sigma)}{\lambda} + \frac{\tau_2(\sigma)}{\lambda^2} \tag{2.36}$$

gives a quasi-steady problem for the leading order term with the solution

$$u_0 = 1 - p(\sigma)\left(\frac{\rho_f}{\rho} - 1\right),$$

where the function p is given implicitly by

$$p = \frac{\sigma^{2/n}}{p^{(1-n)/n}\rho_f^{1/n} + \sigma^{(2-n)/n}(\rho_f - \sigma)}.$$

The moving boundary is then determined as the solution to the nonlinear ordinary differential equation

$$\frac{\mathrm{d}\tau_0}{\mathrm{d}\sigma} = -\left(-\frac{\mathrm{d}\tau_0}{\mathrm{d}\sigma}\right)^{(n-1)/n} - \sigma + \frac{\sigma^2}{\rho_f}$$

with the initial condition $\tau_0 = 0$ at $\sigma = \rho_f$. For the special case $n = 1$ we can integrate directly to find

$$u_0 = 1 - \frac{\sigma^2}{\rho_f + \sigma(\rho_f - \sigma)}\left(\frac{\rho_f}{\rho} - 1\right), \quad \tau_0 = \rho_f - \sigma + \frac{1}{2}(\rho_f - \sigma)^2 - \frac{1}{3\rho_f}(\rho_f - \sigma)^3. \tag{2.37}$$

Results equivalent to the above are detailed in Lin et al. [29], but no further results for $\lambda \gg 1$ are presented in that study.

In order to continue to higher order terms (and subsequent time scales), we set $n = 1$ for the remainder of this section. The remaining problems for u_1 and u_2 are linear, leading to

$$\begin{aligned} u_1 = &-\frac{\sigma(\sigma+2)\rho_f^2(2\rho_f - \rho)(\rho_f - \rho)}{6(\rho_f + \sigma(\rho_f - \sigma))^3} + \left(\frac{1}{\rho} - \frac{1}{\rho_f}\right) \\ &\times \frac{\sigma^2\rho_f^3\left[\sigma^4 - 3\sigma^3\rho_f + \sigma^2(2\rho_f^2 - 3\rho_f + 2) + 4\sigma\rho_f^2 - 6\rho_f\right]}{6(\rho_f + \sigma(\rho_f - \sigma))^4}, \end{aligned} \tag{2.38}$$

$$\tau_1 = \frac{(\rho_f - \sigma)^2}{6}\left(1 + \frac{2\sigma}{\rho_f + \sigma(\rho_f - \sigma)}\right), \tag{2.39}$$

with u_2 and τ_2 not included here due to restrictions on space (the formulae taking up most of one page).

To demonstrate how well these approximations work, we compare in Figure 2.2 some numerical results computed for $\lambda = 10$ and $\mu = 0.1$ with the asymptotic formulae (2.37)–(2.39). We see that even for this moderately large value of λ, the comparison is remarkably good, except for times close to t_e.

We emphasize that we cannot take the limit $\mu \to 0^+$ in the above to check with known results for the case $\mu = 0$, as this time scale does not appear in the $\mu = 0$ problem. On the other hand, we may check that the results are consistent with subsection 2.3 by rewriting τ_0, τ_1, and τ_2 in terms of s and expanding as $s \to 1^-$ to give

$$\begin{aligned} \tau_0 &= \frac{\lambda}{\mu^2}\left\{\mu(1-s) + \frac{1}{2}\lambda(1-s)^2 - \frac{1}{3}\lambda(1-s)^3\right\}, \\ \frac{\tau_1}{\lambda} &= \frac{\lambda}{\mu^2}\left\{\frac{1}{2}(1-s)^2 - \frac{\lambda+\mu}{3\mu}(1-s)^3 + \mathcal{O}((1-s)^4)\right\}, \\ \frac{\tau_2}{\lambda^2} &= \frac{\lambda}{\mu^2}\left\{-\frac{1}{3\mu}(1-s)^3 + \mathcal{O}((1-s)^4)\right\}. \end{aligned}$$

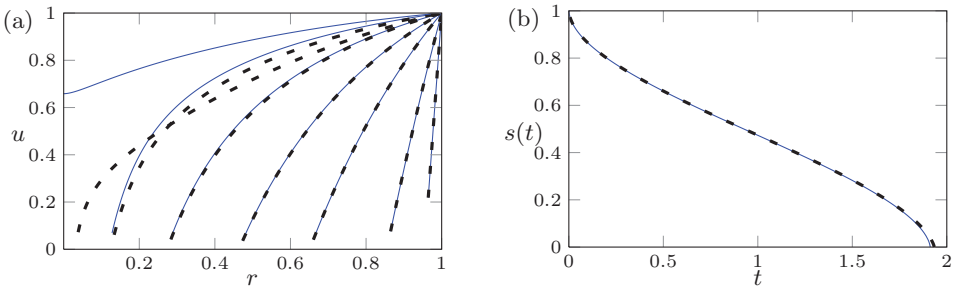

FIG. 2.2. *A comparison of the numerical solution of* (2.6)–(2.10) *(solid) computed for* $\lambda = 10$ *and* $\mu = 0.1$ *with the asymptotic results* (2.37)–(2.39) *(dashed).* (a) *From right to left, profiles of solvent concentration* u *versus radius* r *are shown for times* $t = 0.01$, 0.1, 0.5, 1, 1.5, 1.8, *and* 1.9124. (b) *Dependence of glassy-rubbery interface* $r = s(t)$ *on time* t.

By combining these expressions with (2.36), we see that they agree with (2.18)–(2.19) when $n = 1$, as expected.

2.5.2. Time scale 2, $t = \mathcal{O}(\lambda)$, $1 - s = \mathcal{O}(1)$. The details of this time scale are almost identical to the $\mu = 0$ case [48]. We rescale time as $t = \lambda\hat{t}$, where $\hat{t} = \mathcal{O}(1)$, and write

$$u \sim \hat{u}_0(r,s) + \frac{\hat{u}_1(r,s)}{\lambda} + \frac{\hat{u}_2(r,s)}{\lambda^2}, \quad \hat{t} \sim \hat{t}_0(s) + \frac{\hat{t}_1(s)}{\lambda} + \frac{\hat{t}_2(s)}{\lambda^2},$$

as $\lambda \to \infty$. Again, the glassy-rubbery interface is moving so slowly that the leading order problem is quasi-steady, and, after some algebra, the results

$$\begin{aligned}
\hat{u}_0 &= \frac{r-s}{(1-s)r},\\
\hat{t}_0 &= \tfrac{1}{2}(1-s)^2 - \tfrac{1}{3}(1-s)^3,\\
\hat{u}_1 &= -\frac{1-r}{6rs(1-s)}\left[1-\left(\frac{1-r}{1-s}\right)^2\right] + \frac{\mu(1-r)}{(1-s)^2 r},\\
\hat{t}_1 &= \mu(1-s) + \tfrac{1}{6}(1-s)^2,\\
\hat{u}_2 &= \frac{1-r}{s^3(1-s)r}\left\{\frac{1}{36}\left[1-\left(\frac{1-r}{1-s}\right)^2\right] + \frac{4s-1}{120}\left[1-\left(\frac{1-r}{1-s}\right)^4\right]\right\}\\
&\quad + \frac{\mu(1-r)}{6s^2(1-s)^2 r}\left[1-(1+2s)\left(\frac{1-r}{1-s}\right)^2\right] - \frac{\mu^2(1-r)}{s(1-s)^3 r},\\
\hat{t}_2 &= \tfrac{1}{3}\mu(1-s) - \frac{1}{45s}(1-s)^2
\end{aligned}$$

are readily deduced. Notice how μ does not appear in the leading order description, meaning that this kinetic parameter has a weak effect on the solution on this time scale. In the limit $\mu \to 0^+$, the above expressions reduce to known results in [48].

Further, as $s \to 1^-$, the correction term $\hat{t}_1/\lambda$ becomes the same size as $\hat{t}_0$, implying that these expansions break down when $1 - s = \mathcal{O}(\mu/\lambda)$ or $t = \mathcal{O}(\mu^2/\lambda)$, the scalings for our first time scale. This is as expected. A simple check shows that these time scales match appropriately.

2.5.3. Time scale 3, $t_e - t = \mathcal{O}(1)$, $s = \mathcal{O}(\lambda^{-1/2})$. The third time scale is for times close to the extinction time t_e, at which the glassy-rubbery interface $r = s(t)$ reaches the center. Here $s = \mathcal{O}(\lambda^{-1/2})$, and so we write $s = \lambda^{-1/2}\bar{s}$ in what follows, where $\bar{s} = \mathcal{O}(1)$. In these latter stages the interface begins to speed up again so that the leading order behavior away from the interface is no longer quasi-steady (although the leading order behavior near the interface is). We shall not go through the work here, as the details are very similar to the $\mu = 0$ case. Instead, we simply summarize the results and refer the reader to [48, 49, 50] for a full description of the issues involved.

There are two spatial regions to consider on this time scale. The inner region is for $r = \mathcal{O}(\lambda^{-1/2})$; thus we use the scaled variable $r = \lambda^{-1/2}\bar{r}$, where $\bar{r} = \mathcal{O}(1)$. It turns out that, as $\lambda \to \infty$,

$$u \sim 1 - \frac{\bar{s}}{\bar{r}} + \left\{ \left(\frac{1}{\bar{s}} - \frac{1}{\bar{r}} \right) \left[\bar{s}^2 - \bar{s} \left(\frac{2}{\pi} \right)^{1/2} \sum_{m=1}^{\infty} \frac{\mathrm{e}^{m^2\pi^2\bar{s}^2/2}}{m} \operatorname{erfc}\left(\frac{m\pi\bar{s}}{\sqrt{2}} \right) - \mu \right] + \frac{\mu}{\bar{s}} \right\} \frac{1}{\lambda^{1/2}}$$

in this region, where the glassy-rubbery interface behaves as

(2.40)
$$t \sim \frac{\lambda}{6} + \frac{1 - 3\bar{s}^2 + 6\mu}{6} + \left[\frac{\bar{s}^3}{3} - \frac{\bar{s}}{3} - \left(\frac{2}{\pi^5} \right)^{1/2} \sum_{m=1}^{\infty} \frac{\mathrm{e}^{m^2\pi^2\bar{s}^2/2}}{m^3} \operatorname{erfc}\left(\frac{m\pi\bar{s}}{\sqrt{2}} \right) - \mu\bar{s} \right] \frac{1}{\lambda^{1/2}}.$$

Here $\operatorname{erfc}(z)$ is the complementary error function [1]. The outer region is for $r = \mathcal{O}(1)$, on which we find

(2.41)
$$u \sim 1 - \left[\left(\frac{1}{r} - 1 \right) \bar{s} + \frac{1}{r} \left(\frac{2}{\pi^3} \right)^{1/2} \sum_{m=1}^{\infty} \frac{\mathrm{e}^{m^2\pi^2\bar{s}^2/2}}{m^2} \operatorname{erfc}\left(\frac{m\pi\bar{s}}{\sqrt{2}} \right) \sin(m\pi r) \right] \frac{1}{\lambda^{1/2}}.$$

Again we see that the kinetic parameter μ has only a weak effect on the solution on this time scale.

By taking the limit $\bar{s} \to 0$ in (2.40), we can approximate the extinction time by

$$t_e = \frac{1}{6}\lambda + \frac{1}{6} + \mu - \frac{\sqrt{2}\zeta(3)}{\pi^{5/2}\lambda^{1/2}} + \mathcal{O}(\lambda^{-1}), \tag{2.42}$$

where $\zeta(z)$ is the Riemann zeta function. By setting $\mu = 0$, all of the above results for the third time scale reduce to those given in [48, 49, 50]. We see that for the regime $\lambda \gg 1$, increasing the kinetic parameter μ simply increases the extinction time by $\mu + \mathcal{O}(\lambda^{-1})$.

2.5.4. Summary. The asymptotic behavior of (2.6)–(2.10) in the limit $\lambda \to \infty$ is much more detailed than the corresponding one-dimensional problem treated in [9, 13, 14, 15, 16]. Indeed, the analysis for the first time scale $t = \mathcal{O}(\mu^2/\lambda)$ is very similar to the one-dimensional problem, while the behavior on the second and third time scales mimics that of the more complicated spherical problem with $\mu = 0$ (analyzed by [48, 49, 50]).

Furthermore, by exploiting limiting properties of Clausen's integral [1], the outer region on the third time scale (2.41) appears to have the solvent concentration at the extinction time behaving as

$$u(r, t_e) \sim 1 - \frac{1}{\lambda^{1/2}} \left[\sqrt{\frac{2}{\pi}} (\ln(1/\pi r) + 1) + \mathcal{O}(r^2) \right] \tag{2.43}$$

as $r \to 0$ [48, 49, 50], implying that the analysis on the third time scale cannot be uniformly valid, as the $\ln(1/r)$ term becomes unbounded at the center of the sphere (reflecting the fact that the limits $r \to 0$ and $\lambda \to \infty$ do not commute). For the case $\mu = 0$, this nonuniformity is resolved on an exponentially short time scale $t_e - t = \mathcal{O}(\exp(-2\sqrt{2\pi}\lambda^{1/2}))$ in [49, 50], with the solvent concentration at the extinction time being expressed for $r \ll 1$ as

$$u(r, t_e) \sim \frac{1}{\psi(r)^2}\left[1 + \frac{(-5 + 6\ln 2)\ln\psi(r) + \mathcal{O}(1)}{\sqrt{2\pi}\lambda^{1/2}\psi(r)}\right] \quad \text{as} \quad \lambda \to \infty, \tag{2.44}$$

where

$$\psi(r) = 1 + \frac{\ln(1/r)}{\sqrt{2\pi}\lambda^{1/2}}$$

(see (3.22) in [49]), while the glassy-rubbery interface propagates as

$$s(t) \sim \frac{\sqrt{2}(t_e - t)^{1/2}}{\lambda^{1/2}\psi((t_e - t)^{1/2})}\left[1 + \frac{(-5 + 6\ln 2)\ln\psi((t_e - t)^{1/2}) + \mathcal{O}(1)}{2\sqrt{2\pi}\lambda^{1/2}\psi((t_e - t)^{1/2})}\right] \tag{2.45}$$

(see (3.23) in [49]). Thus for $1 \ll \ln(1/r) \ll \sqrt{2\pi}\lambda^{1/2}$, (2.44) reduces to (2.43), while for $\ln(1/r) \gg \sqrt{2\pi}\lambda^{1/2}$ we have, to leading order,

$$u(r, t_e) \sim \frac{2\pi\lambda}{\ln^2(1/r)} \quad \text{as} \quad r \to 0, \tag{2.46}$$

which implies $u(0, t_e) = 0$, as required in the $\mu = 0$ case. Further, for $1 \ll \ln(1/(t_e - t)) \ll 2\sqrt{2\pi}\lambda^{1/2}$, (2.45) agrees with (2.40) and (2.42), while for $\ln(1/(t_e - t)) \gg 2\sqrt{2\pi}\lambda^{1/2}$, (2.45) has

$$s \sim \frac{4\sqrt{\pi}(t_e - t)^{1/2}}{\ln(1/(t_e - t))} \quad \text{as} \quad t \to t_e^- \tag{2.47}$$

to leading order.

Of particular interest here are the observations that

$$\text{as} \quad r \to 0, \qquad \frac{\partial u(r, t_e)}{\partial r} \to \infty, \tag{2.48}$$

$$\text{as} \quad t \to t_e^-, \qquad \frac{\mathrm{d}s}{\mathrm{d}t} \to -\infty \tag{2.49}$$

when $\mu = 0$. In other words, both the flux of solvent on the interface and the speed of the interface itself become unbounded in the limit $t \to t_e^-$. It is well known that in the context of Stefan problems, kinetic undercooling acts to regularize such singularities, suggesting that (2.48)–(2.49) will no longer hold for the case $\mu > 0$. Indeed, it appears that the $\mu = 0$ analysis for $t_e - t = \mathcal{O}(\exp(-2\sqrt{2\pi}\lambda^{1/2}))$ will not carry over to the case $\mu > 0$.

In general terms, we can summarize by observing that for early times the kinetic parameter μ has quite a significant effect on the process of solvent diffusion, with the qualitative behavior for $\mu > 0$ very different from that for $\mu = 0$, while for later times the effect decreases to the extent that the leading order behavior as $\lambda \to \infty$ does not depend on μ at all on the second and third time scales. On the other hand, we expect that for times extremely close to the extinction time t_e, the solution with $\mu > 0$ will very quickly diverge from the solution with $\mu = 0$, as the kinetic parameter should act to keep the flux of solvent and speed of the interface bounded for all time. With this in mind, we shall consider the limit $t \to t_e^-$ in the following subsection.

2.6. The "extinction limit" $t \to t_e^-$. As mentioned above, for the special case $\mu = 0$, the solvent penetration problem (2.6)–(2.10) reduces to the classical Stefan problem for melting an ice-ball. In that case the results (2.46)–(2.47) are generic in the sense that they hold for all values of λ and not just for $\lambda \gg 1$, as described in the previous subsection (see Herrero and Velázquez [22] as well as [4, 33, 49, 50]). Thus we see that for $\mu = 0$, the limiting behavior (2.48)–(2.49) means that there is an unphysical singularity in the limit $t \to t_e^-$ for all λ. It is known that the addition of surface tension (via the Gibbs–Thomson condition) does not regularize this singularity [35, 53] (in fact, it makes it worse, with the model including surface tension breaking down at a finite time before the interface reaches the center of the ball), so in this context it is of interest to explore the effect that (an alternative regularization) kinetic undercooling $\mu > 0$ has on the Stefan problem.

Numerical solutions of solvent concentration are given in Figure 2.3 for the representative value $\lambda = 1$. In part (a), which is for $\mu = 0$ (corresponding to the classical Stefan problem), the profile at $t = t_e$ does appear to have an infinite slope at $r = 0$, as expected, while in part (b), which is for $\mu = 0.01$, the slope of $u(r, t_e)$ at $r = 0$ is finite.

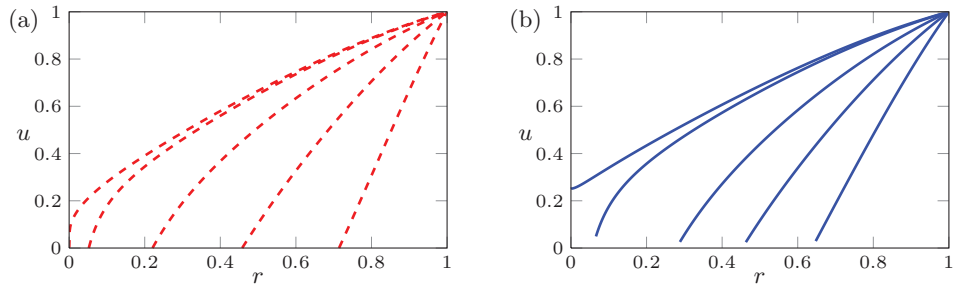

FIG. 2.3. *Profiles of solvent concentration computed for* $\lambda = 1$. (a) $\mu = 0$. (b) $\mu = 0.01$.

Figure 2.4 provides a close-up view of the solutions near $r = 0$, clearly showing that the kinetic parameter $\mu > 0$ regularizes the flux singularity at $t = t_e$. By observing plots (not shown here) of the interface velocity ds/dt versus time close to the extinction time $t = t_e$, we see that the ds/dt remains finite at $t = t_e$ for all $\mu > 0$, no matter how small, meaning that the singular speed that occurs for $\mu = 0$ appears to also be regularized by the addition of the kinetic term.

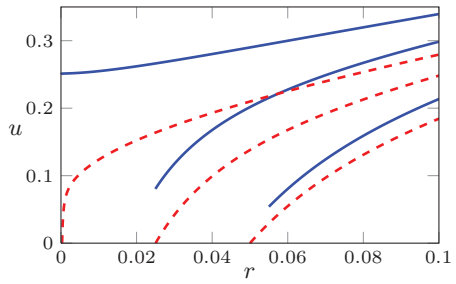

FIG. 2.4. *A comparison of solvent concentration profiles for* $\lambda = 1$ *near the extinction time* $t = t_e$ *for* $s = 0$, 0.025, *and* 0.05. *The dashed profiles are computed with* $\mu = 0$ *and the solid profiles with* $\mu = 0.01$.

Analytically, we can make some progress by rescaling near the glassy-rubbery interface using $\hat{\rho} = r/s$ and writing

$$u \sim \Phi(\hat{\rho}, s) \quad \text{as} \quad s \to 0$$

for $r = \mathcal{O}(s)$. To leading order (2.6), (2.8)–(2.9) gives

$$\Phi = s\dot{s}\left(\lambda + \mu^{1/n}(-\dot{s})^{1/n}\right)\left(\frac{1}{\hat{\rho}} - 1\right) + \mu^{1/n}(-\dot{s})^{1/n}, \tag{2.50}$$

where here $\dot{s} < 0$ denotes the velocity of the interface. If we write $s \sim -\dot{s}_{\rm e}(t_{\rm e} - t)$ as $t \to t_{\rm e}^-$, where $\dot{s}_{\rm e}$ is a constant (cf. (2.47) and (2.49)), one observation from (2.50) is that while the slope $\partial\Phi/\partial\hat{\rho}$ remains nonzero on the interface $\hat{\rho} = 1$ for times leading up to the extinction time, we have $\partial\Phi/\partial\hat{\rho}(1, s) = 0$ at the precise moment of extinction $s = 0$ ($t = t_{\rm e}$), so that

$$u(r, t_{\rm e}) \sim \mu^{1/n}(-\dot{s}_{\rm e})^{1/n} + \mathcal{O}(r^2) \quad \text{as} \quad r \to 0^+,$$

which is in stark contrast to the $\mu = 0$ case (2.46) and (2.48).

It is worth stating that the near-extinction analysis by Herrero and Velázquez [22] and Soward [49] for the case $\mu = 0$ cannot be simply extended to included the effects of the kinetic parameter $\mu > 0$. In that case, by defining $\bar{R} = \ln(1/r)$, $\bar{T} = \ln(1/(t_{\rm e} - t))$, $u(r, t_{\rm e}) = \Theta(\bar{R})$, and $s(t) = (t_{\rm e} - t)^{1/2}\bar{S}(\bar{T})$, a vital part of the analysis is that

$$\Theta(\bar{R}) \gg \frac{{\rm d}\Theta}{{\rm d}\bar{R}} \gg \frac{{\rm d}^2\Theta}{{\rm d}\bar{R}^2} \gg \dots$$

for $\bar{R} \gg 1$ (that is, for $r \ll 1$) and

$$\bar{S}(\bar{T}) \gg \frac{{\rm d}\bar{S}}{{\rm d}\bar{T}} \gg \frac{{\rm d}^2\bar{S}}{{\rm d}\bar{T}^2} \gg \dots$$

for $\bar{T} \gg 1$ (that is, for $t_{\rm e} - t \ll 1$). These assumptions no longer hold when $\mu > 0$.

3. Model for drug diffusion from polymeric spheres.

3.1. Mathematical formulation and numerical results. In section 2 we considered a moving boundary problem (2.1)–(2.4) for solvent penetration through a polymer ball, where (reverting back to dimensional variables) the solvent concentration $U(R, T)$ is governed by a linear diffusion equation in the region $S(T) < R < S(0)$, where $R = S(T)$ describes the location of the interface between the glassy and rubbery regions of polymer. In this section we now suppose that the drug has been dissolved in the polymer matrix and is released from the polymer when it is in a rubbery state (but not released when the polymer is in a glassy state).

By denoting the drug concentration by $V(R, T)$, the problem we are concerned with is

$$\text{in} \quad S(T) < R < S(0), \qquad \frac{\partial V}{\partial T} = \frac{1}{R^2}\frac{\partial}{\partial R}\left(R^2\bar{D}_d(U)\frac{\partial V}{\partial R}\right), \tag{3.1}$$

$$\text{on} \quad R = S(0), \qquad V = 0, \tag{3.2}$$

$$\text{on} \quad R = S(T), \qquad \bar{D}_d(U)\frac{\partial V}{\partial R} = (V_i - V)\frac{{\rm d}S}{{\rm d}T}, \tag{3.3}$$

where the location of the interface $R = S(T)$ is an input to the problem (given by the solution of (2.1)–(2.4), which is not dependent on V). Here (3.2) states that the drug concentration is assumed to vanish on the outer boundary of the polymer ball (the perfect sink condition), while (3.3) is required to conserve the mass of drug in the system. Initially the concentration of the drug is the constant $V(R,0) \equiv V_i$. Following [17, 41, 46], for example, we suppose the nonlinear diffusion coefficient is given by

$$\bar{D}_d(U) = \bar{\delta} \mathrm{e}^{-\bar{\beta}(1-U/U_0)},$$

which is an increasing function of U that reduces to a constant for $\bar{\beta} = 0$. In other words, for $\bar{\beta} = 0$ we have the concentration of the drug governed by the linear diffusion equation, while for $\bar{\beta} > 0$ we suppose that the drug tends to diffuse more in regions of higher concentration of solvent.

We nondimensionalize (3.1)–(3.3) by applying (2.5) and introducing the dimensionless drug concentration $v(r,t) = V/V_i$, resulting in

$$\text{in} \quad s(t) < r < 1, \qquad \frac{\partial v}{\partial t} = \frac{1}{r^2}\frac{\partial}{\partial r}\left(r^2 D_d(u)\frac{\partial v}{\partial r}\right), \tag{3.4}$$

$$\text{on} \quad r = 1, \qquad v = 0, \tag{3.5}$$

$$\text{on} \quad r = s(t), \qquad D_d(u)\frac{\partial v}{\partial r} = (1-v)\frac{\mathrm{d}s}{\mathrm{d}t}, \tag{3.6}$$

where the dimensionless nonlinear diffusion coefficient is given by

$$D_d(u) = \delta \mathrm{e}^{-\beta(1-u)}. \tag{3.7}$$

Equations (3.4)–(3.7) contain two new dimensionless parameters

$$\delta = \frac{\bar{\delta}}{D}, \quad \beta = \bar{\beta}\left(1 - \frac{U^*}{U_0}\right). \tag{3.8}$$

Here δ is the ratio of the diffusion coefficient of the drug on the surface of the ball to the diffusion coefficient of the solvent in the rubbery region. Typically δ is a small parameter; we take $\delta = 0.1$ for all the calculations in the present study. The other parameter, β, measures the strength of the nonlinearity of the diffusion of the drug, with (3.4) reducing to the linear diffusion equation for the special case $\beta = 0$.

It is important to note that once the glassy-rubbery interface reaches the center, the polymer ball will be entirely in the rubbery state, but the drug will continue to be released. For $t > t_\mathrm{e}$ we continue to solve (3.4), except the domain is changed to $0 < r < 1$, together with boundary conditions (3.5) and

$$\text{on} \quad r = 0, \quad \frac{\partial v}{\partial r} = 0. \tag{3.9}$$

That is, for $t > t_\mathrm{e}$ this is no longer a moving boundary problem.

To summarize, the problems for concentrations of solvent and drug are partially coupled in the sense that we may solve (2.6)–(2.10) given the two parameters defined in (2.11) and then use this solution as an input for (3.4)–(3.7), which requires the two extra parameters (3.8). Collectively, (2.6)–(2.10) and (3.4)–(3.7) are very similar to the problem treated in Lin and Peng [30], except for two differences: first, in [30] the parameter $\beta = 0$, so those authors do not consider the effect that solvent has on the diffusion coefficient for the drug; second, the model considered by Lin and Peng

allows the polymer matrix to swell, leading to a double moving boundary problem that is the radially symmetric extension of the one-dimensional model proposed by Cohen and Erneux [10]. We shall mention the effects of swelling briefly in section 4 but note for now that provided the molar volume of the solvent is small compared to $1/U_0$, all of the results presented here are qualitatively the same as those for the more complicated double moving boundary problem.

Of particular concern for those working in the pharmaceutical industry is to calculate the quantity

$$m_t = -3\delta \int_0^t \left.\frac{\partial v}{\partial r}\right|_{r=1} \mathrm{d}t, \tag{3.10}$$

which is the dimensionless amount of drug released from the spherical delivery device at time t, normalized so that $m_t \to 1^-$ as $t \to \infty$ (that is, m_t is the ratio of the drug released at time t to the amount of the drug in the polymer at $t = 0$).

Typical numerical results are presented in Figure 3.1. The plots in parts (a) and (c) come from solving (2.6)–(2.10) for the parameter values $\lambda = 0.8$ and $\mu = 0.1$, as described in section 2.4. The dashed curve in (a) denotes the profile of solvent concentration at the extinction time t_e; for latter times the domain is fixed and the relevant equations are (2.6) (with the domain changed to $0 < r < 1$), (2.7), and (2.12), as discussed in section 2.1. Figures 3.1(b) and (d) contain numerical results of (3.4)–(3.7) for $\delta = 0.1$ and $\beta = 20$, where $u(r,t)$ and $s(t)$ are found from the numerical solution to (2.6)–(2.10). The numerical scheme for solving (3.4)–(3.7) is a straightforward extension of that described in section 2.4 and will not be elaborated on here.

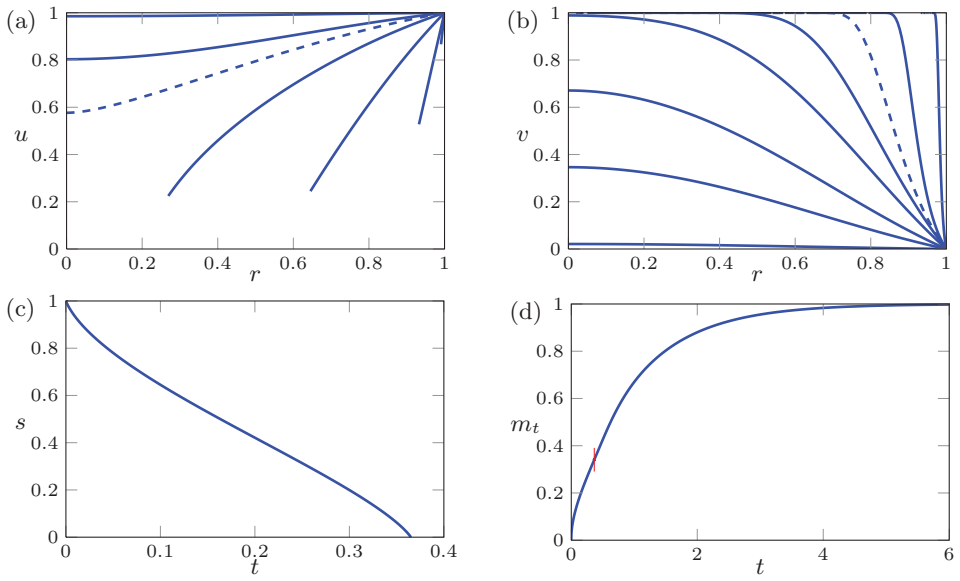

FIG. 3.1. *Numerical results for* $\lambda = 0.8$, $\mu = 0.1$, $\delta = 0.1$, *and* $\beta = 20$. (a) *From right to left, profiles of solvent concentration* $u(r,t)$ *are shown for* $t = 0.001$, 0.01, 0.1, 0.27, 0.3651 *(dashed),* 0.4201, *and* 0.6801. (b) *From right to left, profiles of drug concentration* $v(r,t)$ *are shown for* $t = 0.01$, 0.17, 0.3651 *(dashed),* 0.5511, 0.8311, 1.4251, 2.1251, *and* 4.9651. (c) *Dependence of glassy-rubbery interface* $r = s(t)$ *on time* t. (d) *Normalized drug release* m_t *versus time* t. *The vertical thin marker indicates the time the interface reaches the center,* $t_e = 0.3651$.

We close this subsection by noting some evidence that we believe highlights how our numerical scheme is preferred to that employed by Lin and Peng [30]. Figure 3.2 shows profiles of flux $-\partial v/\partial r$ at $r = 1$ for time, which for $\beta = 0$ is a measure of drug being released from the outer surface of the polymer ball. Note how the curves are monotonically decreasing, which is as expected given that the solution for $v(r,t)$ becomes flatter and tending to $v(r,t) \equiv 0$ as time increases. This monotonic behavior is in contrast to the numerical results shown in [30], where a number of profiles of the flux $-\partial v/\partial r(1,t)$ versus time are presented, but each has a distinct local minimum followed by a sharp rise just before $t = t_e$.

As a check on our scheme, we computed the normalized drug release m_t defined in (3.10) for a variety of parameter sets (including those presented in [30]) and found that, for large times, m_t approaches 1 (as expected) to within at least 3 decimal places. This is a strong test, as any small numerical error in calculating the flux $-\partial v/\partial r(1,t)$ accumulates in time when computing m_t. The apparent inaccuracy of the numerical scheme in [30] is not surprising, since it relies on an approximate similarity solution on each time step that becomes less and less accurate as time increases; indeed, in the limit $t \to t_e^-$, the similarity solution used in [30] is not even a rough approximation of the real behavior exhibited by (2.6)–(2.9), (3.4)–(3.7).

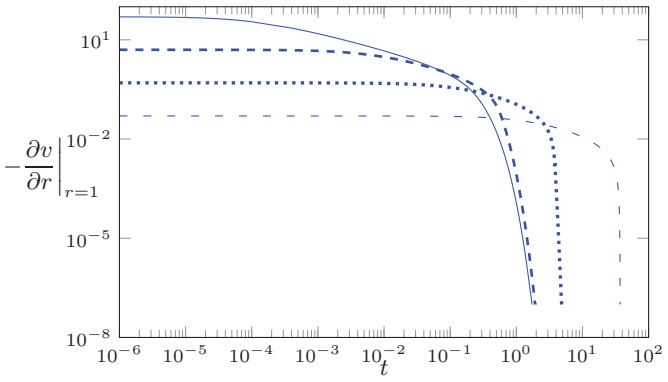

FIG. 3.2. *Profiles of the flux of drug at the surface of the polymer ball versus time calculated for $\delta = 1$, $\beta = 0$. The solid line is for $\lambda = 0.1$, $\mu = 0.02$, the dashed line for $\lambda = 1$, $\mu = 0.2$, the dotted line for $\lambda = 10$, $\mu = 2$, and the loosely dashed line for $\lambda = 100$, $\mu = 20$. These parameter values are the same as those used in Figure 13 of [30], except that those authors have included the effects of swelling as the solvent penetrates the polymer ball. Such effects, which do not change the qualitative behavior of drug release, are ignored in our model.*

3.2. Asymptotic limits. We can derive a small-time expansion for drug concentration v by applying the ansatz

$$v \sim \frac{1}{r}\{v_0(\xi) + v_1(\xi)(1-s) + v_2(\xi)(1-s)^2\} \quad \text{as} \quad s \to 1^-$$

(together with (2.17)–(2.18)), where ξ is the front-fixing variable defined in (2.16). The result is that

$$v \sim \frac{1}{\delta\mu}\left(\frac{1-r}{r}\right) + \frac{\beta(1+\lambda)}{2\delta\mu^2}\left(\frac{(1-r)^2}{r}\right) - \frac{1+2\delta\mu+\delta n(1+\lambda)}{\delta^2\mu^3}\left(\frac{1-r}{r}\right)t \tag{3.11}$$

as $t \to 0^+$. We can thus deduce that

$$\left.\frac{\partial v}{\partial r}\right|_{r=1} \sim -\frac{1}{\delta\mu} + \frac{1+2\delta\mu+\delta n(1+\lambda)}{\delta^2\mu^3}\, t, \tag{3.12}$$

$$m_t \sim \frac{3}{\mu}\, t - \frac{3[1+2\delta\mu+\delta n(1+\lambda)]}{2\delta\mu^3}\, t^2 \tag{3.13}$$

as $t \to 0^+$.

These results provide a modest contribution to the literature (the small-time analysis of (2.6)–(2.10) and (3.4)–(3.7) was not attempted in [30]) but are of considerable interest given the vast amount of attention given to the rate of drug release in the past. Equations (3.12)–(3.13) show explicitly how the flux of drug from the polymer ball is $\mathcal{O}(1)$ and the normalized drug release is $\mathcal{O}(t)$ in the small-time limit, and the effect the kinetic parameter μ has on these processes. In particular, the kinetic boundary condition (2.9) (which leads to the so-called Case II diffusion of solvent through the polymer) dictates the scalings of drug release for small time, and without this empirical law the time-dependence would be qualitatively different (as in [26, 39, 41, 51, 52], for example). Clearly (3.12)–(3.13) break down in the limit $\mu \to 0^+$, and in fact (3.11)–(3.13) are valid only for $t = \mathcal{O}(\mu^2)$ in this limit (see the related discussion in section 2.3). This implies that for $\mu = 0$ the above analysis no longer holds; indeed, for $\mu = 0$ we find that $\partial v/\partial r(r,1) = \mathcal{O}(t^{-1/2})$ and $m_t = \mathcal{O}(t^{1/2})$ as $t \to 0^+$ (for $\beta = 0$ we have

$$m_t \sim \frac{6\alpha e^{\alpha^2/\delta}}{1+\alpha\sqrt{\pi/\delta}e^{\alpha^2/\delta}\mathrm{erf}(\alpha/\sqrt{\pi})}\, t^{1/2} \quad \text{as} \quad t \to 0^+,$$

where α is the positive real root of (2.29)). Thus, it happens that if (2.9) is replaced by the condition $u = 0$ on $r = s(t)$, then the early drug release scales the same way as predicted by Higuchi [23] or even a simple linear model (see section 3.3 below).

For the case $n = 1$ it is possible to extend the large-λ analysis of (2.6)–(2.10) in section 2.5 to take into account the drug diffusion problem (3.4)–(3.7), although the algebra is tedious. For brevity we simply note that on the first time scale $t = \mathcal{O}(\mu^2/\lambda)$ we rescale variables as in (2.34)–(2.35) and find for $\beta = 0$ the leading order solution

$$v \sim \frac{1}{\delta\lambda}\left(\frac{\rho_f}{\rho} - 1\right)\frac{\sigma^2}{\rho_f + \sigma(\rho_f - \sigma)} \quad \text{as} \quad \lambda \to \infty,$$

where σ and τ are related by $(2.36)_2$ and $(2.37)_2$ (this term was given in [30]). By integrating (3.10) we find that

$$m_t \sim \frac{\mu}{\lambda\rho_f^2}(\rho_f^3 - \sigma^3) \quad \text{as} \quad \lambda \to \infty,$$

again to leading order. Interestingly, by writing in original variables, this provides the very simple approximation

$$m_t \approx 1 - s^3 \quad \text{for} \quad \lambda \gg 1.$$

Since $s \sim 1 - t/\mu$ as $t \to 0^+$, this reduces further to

$$m_t \sim 3(1-s) \sim \frac{3}{\mu}\, t \quad \text{as} \quad t \to 0^+, \quad \lambda \to \infty,$$

which agrees with the small-time expansion (3.13) (valid for all λ), as expected.

3.3. Comparison with the linear model. It is instructive to compare the results for the problem (2.6)–(2.10), (3.4)–(3.7) with those for the linear initial boundary value problem

$$\text{in} \quad 0 < r < 1, \qquad \frac{\partial v}{\partial t} = \delta \frac{1}{r^2} \frac{\partial}{\partial r} \left(r^2 \frac{\partial v}{\partial r} \right), \tag{3.14}$$

$$\text{on} \quad r = 1, \qquad v = 0, \tag{3.15}$$

$$\text{on} \quad r = 0, \qquad \frac{\partial v}{\partial r} = 0, \tag{3.16}$$

$$\text{at} \quad t = 0, \qquad v = 1. \tag{3.17}$$

Equations (3.14)–(3.17) provide the most simple nontrivial description of genuine drug diffusion from a spherical delivery device where the drug is initially uniformly dissolved in the polymer ball (see [5], for example). The model has linear diffusion in the fixed domain $0 < r < 1$ (without a moving boundary) and does not take into account any effects of solvent. The only parameter is δ, the constant diffusion coefficient (which could be scaled out of (3.14)–(3.17) but is kept here to be consistent with previous scalings).

By separating variables or applying a Laplace transform, (3.14)–(3.17) may be solved exactly to give [11]

$$\begin{aligned} v(r,t) &= \frac{2}{\pi} \sum_{m=1}^{\infty} \frac{(-1)^{m+1}}{m} \frac{\sin(m\pi r)}{r} \mathrm{e}^{-m^2\pi^2\delta t} \\ &= 1 + \frac{1}{r} \sum_{m=0}^{\infty} \left\{ \operatorname{erfc}\left(\frac{2m+1+r}{2\sqrt{\delta t}} \right) - \operatorname{erfc}\left(\frac{2m+1-r}{2\sqrt{\delta t}} \right) \right\}, \end{aligned}$$

with the normalized drug release given by

$$\begin{aligned} m_t &= 1 - \frac{6}{\pi^2} \sum_{m=1}^{\infty} \frac{1}{m^2} \mathrm{e}^{-m^2\pi^2\delta t} \\ &= 6\sqrt{\frac{\delta t}{\pi}} - 3\delta t + 12 \sum_{m=1}^{\infty} \left\{ \sqrt{\frac{\delta t}{\pi}} \mathrm{e}^{-m^2/\delta t} - m \operatorname{erfc}\left(\frac{m}{\sqrt{\delta t}} \right) \right\}. \end{aligned}$$

An obvious qualitative difference between this solution and the solution to (2.6)–(2.10), (3.4)–(3.7) is that

$$m_t \sim \frac{6\sqrt{\delta}}{\sqrt{\pi}} t^{1/2} \quad \text{as} \quad t \to 0^+ \tag{3.18}$$

for the linear problem (3.14)–(3.17), meaning that $m_t = \mathcal{O}(t^{1/2})$ as $t \to 0^+$, whereas from (3.13) we see that $m_t = \mathcal{O}(t)$ for the full moving boundary problem. Thus the linear problem (3.14)–(3.17), which makes no reference to either solvent or the glassy-rubbery interface, does not provide a small-time drug release rate that scales the same way as our model, which has the interface kinetics governed by an empirical law relating the concentration of solvent there to the velocity of the interface.

While these observations are important, we have found that for certain parameter regimes the solution to the linear problem (3.14)–(3.17) provides a very good approximation to (2.6)–(2.10), (3.4)–(3.7) for times away from $t = 0$. For example,

the dependence of the normalized drug release on time is presented in Figure 3.3 for fixed values of μ and δ and $\beta = 0$ but three different values of the control parameter λ. We see that for $\lambda = 1$ the comparison is very good, except for very small times. While not shown here, the comparison was found to improve even further as λ decreases. The explanation for this agreement is that for small values of λ the glassy-rubbery interface moves quickly and reaches the center of the ball before much of the drug is released. From that time the problem for drug concentration is (3.4) (with the domain replaced by $0 < r < 1$), (3.5), and (3.9), which for $\beta = 0$ coincides with (3.14)–(3.17). On the other hand, for large values of λ (see the drug release profile in Figure 3.3 for $\lambda = 50$), the glassy-rubbery interface moves very slowly, and almost all the drug is released before $t = t_e$. For this parameter regime the comparison with the linear problem (3.14)–(3.17) is not good at all (but in terms of an analytical approximation, we are able to resort to our large λ asymptotics in that case).

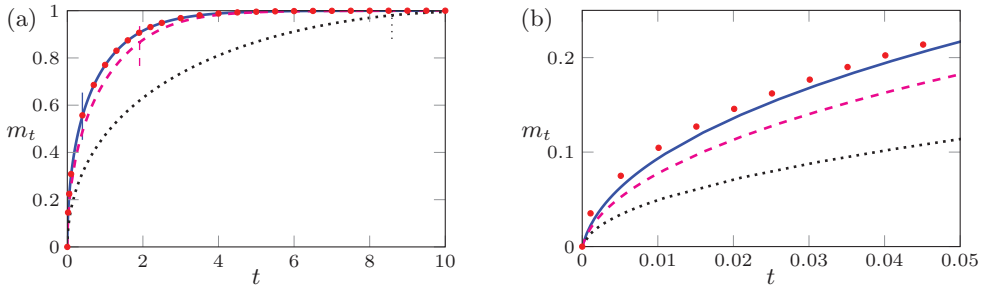

FIG. 3.3. *Normalized drug release m_t versus t for $\mu = 0.1$, $\delta = 0.1$, $\beta = 0$ and for $\lambda = 1$ (solid line), 10 (dashed line), and 50 (dotted line). The solid, dashed, and dotted vertical markers indicate the time t_e for the cases $\lambda = 1$, 10, and 50, respectively. Also included, as solid circles, is the solution of the linear diffusion problem for $\delta = 0.1$.*

Similar observations can be made for other parameter regimes. For example, in Figure 3.4 we see that for $\beta = 0$ and small values of the kinetic parameter μ, the linear problem (3.14)–(3.17) provides a very good approximation of the full moving boundary problem (2.6)–(2.10), (3.4)–(3.7), except for very small times.

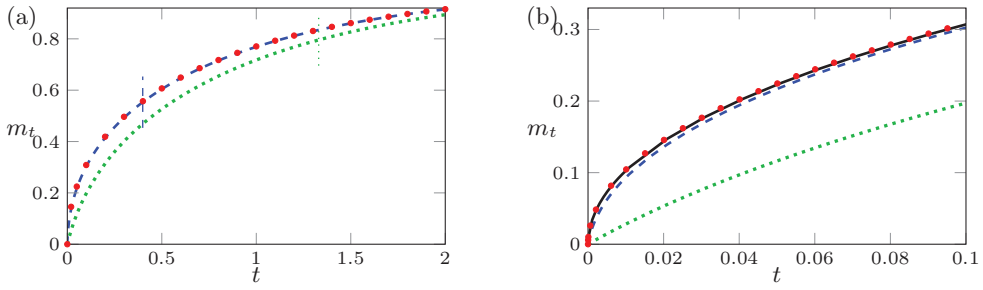

FIG. 3.4. *Normalized drug release m_t versus t for $\lambda = 1$, $\delta = 0.1$, $\beta = 0$ and for $\mu = 0$ (solid line), 0.1 (dashed line), and 1 (dotted line). The dashed and dotted vertical markers indicate the time t_e for the cases $\mu = 0.1$ and 1, respectively. Also included, as solid circles, is the solution of the linear diffusion problem for $\delta = 0.1$.*

In Figure 3.5 we see that increasing the effects of nonlinear diffusion of the drug (by increasing β) moves the drug release profile away from the linear profile. That is to

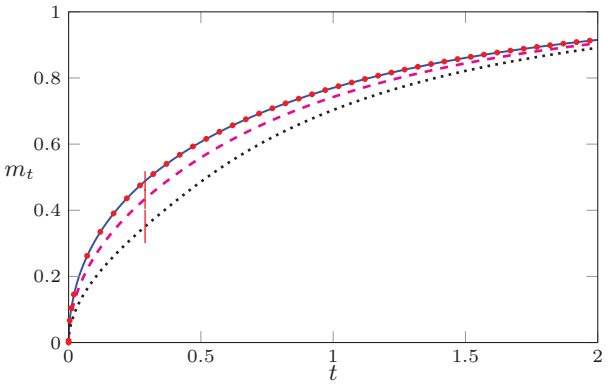

FIG. 3.5. *Normalized drug release m_t versus t for $\lambda = 1$, $\mu = 0.01$, $\delta = 0.1$ and for $\beta = 0$ (solid line), 5 (dashed line), and 20 (dotted line). The thin vertical marker indicates the time t_e for these profiles. Also included, as solid circles, is the solution of the linear diffusion problem for $\delta = 0.1$.*

say, for large β the linear problem (3.14)–(3.17) does not provide a good approximation of the full moving boundary problem (2.6)–(2.10), (3.4)–(3.7).

3.4. Multilayered system. Instead of having an evenly distributed amount of drug initially dissolved in the polymer, it is possible to construct a drug delivery device with different levels of initial drug concentration in different regions. Perhaps the most simple example which is an extension of our model is to assume that, instead of having $u(r, 0) = 1$ for all r, we have

$$u(r,0) = \begin{cases} 1, & 0 < r < r_\ell, \\ 0, & r_\ell < r < 1. \end{cases} \tag{3.19}$$

That is, we suppose that the drug is evenly dissolved in the core of the polymer ball $0 < r < r_\ell$, but no drug is initially stored in the outer shell $r_\ell < r < 1$. Otherwise, the governing equations (2.6)–(2.10), (3.4)–(3.7) remain the same, with the same alterations once the glassy-rubbery interface reaches the center.

In Figure 3.6 we present typical numerical results for such a two-layered device. The value $r_\ell = 2^{-1/3} \approx 0.7937$ implies that the inner core initially containing the drug is one half of the volume of the polymer ball. Parts (a) and (b) show profiles of solvent and drug concentration for various times, respectively. Here the dotted curve represents the time at which the glassy-rubbery interface reaches the inner core (that is, the solvent concentration profile at which $s = r_\ell$), while the dashed curve represents the time at which the interface reaches the center.

To demonstrate the effect that this simple multilayered device has on the drug release rate, we have included plots of normalized drug release versus time in Figure 3.7 for three cases. The first case is for $r_\ell = 1$, which is simply the one-layered device treated in the bulk of this paper. The second case is for two polymer balls with $r_\ell = 2^{-1/3}$, while the third is for three polymer balls with $r_\ell = 3^{-1/3}$. Note that the same amount of drug is released in each case, with the same parameter values except r_ℓ. It is immediately clear that the rate of drug release is greatly affected by dissolving the drug in a multilayered device, and, depending on the application in mind, it is easy to imagine that one could construct a multilayered device that is able to provide a release rate that is desirable. We leave this exercise for further research.

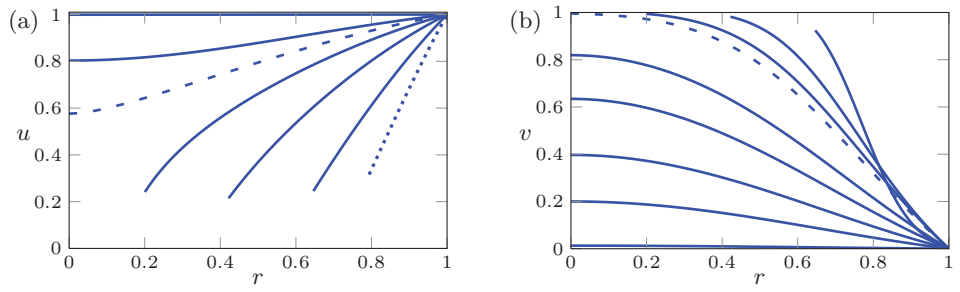

FIG. 3.6. *Profiles of solvent and drug concentration in a two-layered controlled released device for* $\lambda = 0.8$, $\mu = 0.1$, $\delta = 0.1$, *and* $\beta = 0$. *Here* $r_\ell = 2^{-1/3}$.

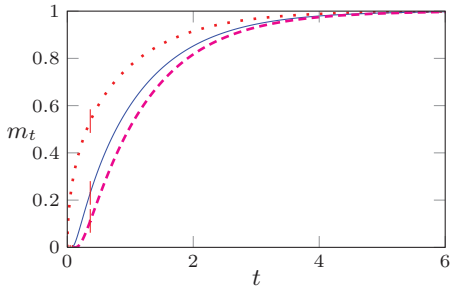

FIG. 3.7. *Normalized drug release* m_t *versus* t *for* $\lambda = 0.8$, $\mu = 0.1$, $\delta = 0.1$, *and* $\beta = 0$, *with the thin vertical markers indicating the extinction time* t_e. *The three cases are one polymer ball with* $r_\ell = 1$ *(dotted line), two polymer balls with* $r_\ell = 2^{-1/3}$ *(solid line), and three polymer balls with* $r_\ell = 3^{-1/3}$ *(dashed line).*

4. Discussion. We have been concerned with the moving boundary problem (2.6)–(2.10), (3.4)–(3.7), which couples together the processes of solvent and drug transport in a spherically shaped glassy polymer. Although (2.6)–(2.10) was considered in [29], where numerical solutions were presented and a leading order term in a large-λ expansion was given on an early time scale, we provide what we believe is a much more accurate numerical scheme and a rather complete asymptotic analysis in the limits $t \to 0^+$, $\lambda \to \infty$, and $t \to t_e^-$. Regarding the full problem (2.6)–(2.10), (3.4)–(3.7), which for $\beta = 0$ was considered in [30], we derive a small-time approximation not attempted by those authors and again provide numerical solutions that we believe are considerably more accurate. Further, we briefly treat a multilayered version of the model, which could be useful for controlling drug release rates.

In our analysis we have found that the kinetic boundary condition (2.9) (the dimensionless version of (2.4)) in the model is crucial in determining the qualitative behavior of the rate of solvent penetration, the speed of the glassy-rubbery interface, and rate of drug release for early times. Much has been made of this issue in the literature, and we emphasize that the model (2.6)–(2.10), (3.4)–(3.7) has $\partial u/\partial r(1,t) = \mathcal{O}(1)$, $\mathrm{d}s/\mathrm{d}t = \mathcal{O}(1)$, and $m_t = \mathcal{O}(t)$ as $t \to 0^+$. From a mathematical perspective, the parameter μ has a regularizing effect in both the limits $t \to 0^+$ and $t \to t_e^-$ in the sense that a model with $\mu = 0$ (that is, if the dimensional kinetic boundary condition (2.4) is replaced with $U = U^*$ on $R = S(T)$) has unphysical singular behavior there, while the full model (2.6)–(2.10), (3.4)–(3.7) with $\mu > 0$ does not.

Our results show that for certain parameter regimes the simple linear problem

(3.14)–(3.17) provides quite a good approximation of the full moving boundary problem (2.6)–(2.10), (3.4)–(3.7). One such regime is when both λ and μ are small and $\beta = 0$; in this case the glassy-rubbery interface moves so quickly that the extinction time t_e is small compared to the time scale on which drug diffuses out of the polymer ball (which, for our choice of dimensionless variables, is $t = \mathcal{O}(1)$), and for subsequent times the full problem becomes linear anyway. The lesson here in terms of mathematical modeling is that one must be careful about spending time developing sophisticated models when sometimes the most obvious formulations are good enough. On the other hand, we have shown that for some parameter regimes (for example, with a slow moving interface, a large kinetic parameter μ, or a highly nonlinear diffusion coefficient), a simple linear model is certainly not appropriate.

Finally, we note that Lin and Peng [30] treat (2.6)–(2.9), (3.4)–(3.7) with the domain $s(t) < r < 1$ replaced with $s_1(t) < r < s_2(t)$, the fixed boundary $r = 1$ replaced with $r = s_2(t)$, and the initial condition $s_1 = s_2 = 1$ at $t = 0$. As there are two moving boundaries $r = s_1(t)$ and $r = s_2(t)$, the extra condition

$$s_2^3(t) - 1 = 3\nu_m \int_{s_1(t)}^{s_2(t)} \left(1 - \frac{1-u}{\lambda+1}\right) r^2 \mathrm{d}r$$

is required, where the dimensionless parameter $\nu_m < 1$ is the molar volume of the solvent multiplied by U_0 (this model is the radially symmetric version of the one proposed in [10]). For practical cases in which the molar volume of solvent is low, there is only a small amount of swelling, and the single moving boundary problem (2.6)–(2.9), (3.4)–(3.7) is a good approximation; indeed, we performed a variety of numerical calculations for the full model with $\nu_m \ll 1$ and found that the results are qualitatively similar to those for $\nu_m = 0$ in [54]. It is of some interest to consider a more complicated model that builds on [30] and to also consider dissolution of polymer on the outer moving boundary $r = s_2(t)$. Such a study will be presented elsewhere.

Acknowledgment. Scott McCue wishes to thank John King for helpful discussions on Stefan problems.

REFERENCES

[1] M. Abramowitz and I. A. Stegun, *Handbook of Mathematical Functions with Formulas, Graphs, and Mathematical Tables*, Dover, New York.

[2] T. Alfrey, E. F. Gurnee, and W. G. Lloyd, *Diffusion in glassy polymers*, J. Polymer Sci. C, 12 (1966), pp. 249–261.

[3] D. Andreucci and R. Ricci, *A free boundary problem arising from sorption of solvents in glassy polymers*, Quart. Appl. Math., 44 (1987), pp. 649–657.

[4] D. Andreucci, M. A. Herrero, and J. J. L. Velázquez, *The classical one-phase Stefan problem: A catalog of interface behaviors*, Surveys Math. Indust., 9 (2001), pp. 247–337.

[5] D. Y. Arifin, L. Y. Lee, and C.-H. Wang, *Mathematical modeling and simulations of drug release from microspheres: Implications to drug delivery systems*, Adv. Drug Delivery Rev., 58 (2006), pp. 1274–1325.

[6] G. Astarita and G. C. Sarti, *A class of mathematical models for sorption of swelling solvents in glassy polymers*, Polymer Eng. Sci., 18 (1978), pp. 388–395.

[7] G. Astarita and S. Joshi, *Sample-dimension effects in the sorption of solvents in polymers: A mathematical mode*, J. Membrane Sci., 4 (1978), pp. 165–182.

[8] C. S. Brazel and N. A. Peppas, *Modeling of drug release from swellable polymers*, Euro. J. Pharm. Biopharm., 49 (2000), pp. 47–58.

[9] D. S. Cohen and T. Erneux, *Free boundary problems in controlled release pharmaceuticals. I: Diffusion in glassy polymers*, SIAM J. Appl. Math., 48 (1988), pp. 1451–1465.

[10] D. S. Cohen and T. Erneux, *Free boundary problems in controlled release pharmaceuticals. II: Swelling-controlled release*, SIAM J. Appl. Math., 48 (1988), pp. 1466–1474.

[11] J. Crank, *The Mathematics of Diffusion*, Oxford University Press, Oxford, UK, 1956.
[12] J. Crank, *Free and Moving Boundary Problems*, Oxford University Press, New York, 1984.
[13] A. Fasano, G. H. Meyer, and M. Primicerio, *On a problem in the polymer industry: Theoretical and numerical investigation of swelling*, SIAM J. Math. Anal., 17 (1986), pp. 945–960.
[14] B. Hu, *Diffusion of penetrant in a polymer: A free boundary problem*, SIAM J. Math. Anal., 22 (1991), pp. 934–956.
[15] J. D. Evans and J. R. King, *Asymptotic results for the Stefan problem with kinetic undercooling*, Quart. J. Mech. Appl. Math., 53 (2000), pp. 449–473.
[16] J. D. Evans and J. R. King, *The Stefan problem with nonlinear kinetic undercooling*, Quart. J. Mech. Appl. Math., 56 (2003), pp. 139–161.
[17] H. Fujita, *Diffusion in polymer-diluent systems*, Fortschr. Hochpolym.-Forsch., 3 (1961), pp. 1–47.
[18] P. Guidotti, *Diffusion in glassy polymers: A free boundary value problem*, Adv. Math. Sci. Appl., 7 (1997), pp. 675–693.
[19] P. Guidotti, *Diffusion in glassy polymers: Sorption of a finite amount of solvent*, NoDEA Nonlinear Differential Equations Appl., 6 (1999), pp. 297–317.
[20] P. Guidotti and J. A. Pelesko, *Transient instability in case* II *diffusion*, J. Polymer Sci. B, 36 (1998), pp. 2941–2947.
[21] D. Hariharan and N. A. Peppas, *Modelling of water transport and solute release in physiologically sensitive gels*, J. Controlled Release, 23 (1993), pp. 123–136.
[22] M. A. Herrero and J. J. L. Velázquez, *On the melting of ice balls*, SIAM J. Math. Anal., 28 (1997), pp. 1–32.
[23] T. Higuchi, *Rate of release of medicaments from ointment bases containing drugs in suspensions*, J. Pharm. Sci., 50 (1961), pp. 874–875.
[24] S. Kiil and K. Dam-Johansen, *Controlled drug delivery from swellable hydroxypropylmethylcellulose matrices: Model-based analysis of observed radial front movements*, J. Controlled Release, 90 (2003), pp. 1–21.
[25] J. R. King and J. D. Evans, *Regularization by kinetic undercooling of blow-up in the ill-posed Stefan problem*, SIAM J. Appl. Math., 65 (2005), pp. 1677–1707.
[26] P. I. Lee and N. A. Peppas, *Prediction of polymer dissolution in swellable controlled-release systems*, J. Controlled Release, 6 (1987), pp. 207–215.
[27] C.-C. Lin and A. T. Metters, *Hydrogels in controlled release formulations: Network design and mathematical modeling*, Adv. Drug Delivery Rev., 58 (2006), pp. 1379–1408.
[28] J.-S. Lin, C.-C. Hwang, J.-Y. Hsieh, and S.-C. Lee, *Swelling controlled release of drug from polymetric delivery devices: A local similarity solution*, J. Phys. Soc. Japan, 7 (2000), pp. 1991–1998.
[29] J.-S. Lin, C.-C. Hwang, C.-M. Lin, and J.-Y. Lai, *Solvent transport in spherical polymer-penetrant systems*, Chem. Eng. Sci., 56 (2001), pp. 151–156.
[30] J.-S. Lin and Y.-L. Peng, *Swelling controlled release of drug in spherical polymer-penetrant systems*, Int. J. Heat Mass Trans., 48 (2005), pp. 1186–1194.
[31] T. C. Illingworth and I. O. Golosnoy, *Numerical solutions of diffusion-controlled moving boundary problems which conserve solute*, J. Comput. Phys., 209 (2005), pp. 207–225.
[32] S. W. McCue, J. R. King, and D. S. Riley, *Extinction behaviour for two-dimensional solidification problems*, R. Soc. Lond. Proc. Ser. A Math. Phys. Eng. Sci., 459 (2003), pp. 977–999.
[33] S. W. McCue, J. R. King, and D. S. Riley, *The extinction problem for three-dimensional inward solidification*, J. Engrg. Math., 52 (2005), pp. 389–409.
[34] S. W. McCue, B. Wu, and J. M. Hill, *Classical two-phase Stefan problem for spheres*, Proc. R. Soc. Lond. Ser. A Math. Phys. Eng. Sci., 464 (2008), pp. 2055–2076.
[35] S. W. McCue, B. Wu, and J. M. Hill, *Micro/nanoparticle melting with spherical symmetry and surface tension*, IMA J. Appl. Math., 74 (2009), pp. 439–457.
[36] A. S. Michaels, H. J. Bixler, and H. B. Hopfenberg, *Controllably crazed polystyrene: Morphology and permeability*, J. Appl. Polymer Sci., 12 (1968), pp. 991–1007.
[37] B. Narasimhan, *Mathematical models describing polymer dissolution: Consequences for drug delivery*, Adv. Drug Delivery Rev., 48 (2001), pp. 195–210.
[38] B. Narasimhan and N. A. Peppas, *The physics of polymer dissolution: Modeling approaches and experimental behavior*, Adv. Polymer Sci., 128 (1997), pp. 157–207.
[39] B. Narasimhan and N. A. Peppas, *Molecular analysis of drug delivery systems controlled by dissolution of the polymer carrier*, J. Pharm. Sci., 86 (1997), pp. 297–304.
[40] N. A. Peppas, R. Gurny, E. Doelker, and P. Buri, *Modelling of drug diffusion through swellable polymeric systems*, J. Membrane Sci., 7 (1980), pp. 241–253.

[41] F. A. Radu, M. Bause, P. Knabner, G. W. Lee, and W. C. Friess, *Modeling of drug release from collagen matrices*, J. Pharm. Sci., 91 (2002), pp. 964–972.
[42] L. F. Shampine and M. W. Reichelt, *The MATLAB ODE suite*, SIAM J. Sci. Comput., 18 (1997), pp. 1–22.
[43] J. Siepmann, H. Kranz, R. Bodmeier, and N. A. Peppas, *HPMC-matrices for controlled drug delivery: A new model combining diffusion, swelling, and dissolution mechanisms and predicting the release kinetics*, Pharm. Res., 16 (1999), pp. 1748–1756.
[44] J. Siepmann and N. A. Peppas, *Hydrophilic matrices for controlled drug delivery: An improved mathematical model to predict the resulting drug release kinetics (the "sequential layer" model)*, Pharm. Res., 17 (2000), pp. 1290–1298.
[45] J. Siepmann and N. A. Peppas, *Modeling of drug release from delivery systems based on hydroxypropyl methylcellulose (HPMC)*, Adv. Drug Delivery Rev., 48 (2001), pp. 139–157.
[46] J. Siepmann, K. Podual, M. Sriwongjanya, N. A. Peppas, and R. Bodmeier, *A new model describing the swelling and drug release kinetics from hydroxypropyl methylcellulose tablets*, J. Pharm. Sci., 88 (1999), pp. 65–72.
[47] J. Siepmann and F. Siepmann, *Mathematical modeling of drug delivery*, Int. J. Pharm., 364 (2008), pp. 328–343.
[48] D. S. Riley, F. T. Smith, and G. Poots, *The inward solidification of spheres and circular cylinders*, Int. J. Heat Mass Trans., 17 (1974), pp. 1507–1516.
[49] A. M. Soward, *A unified approach to Stefan's problem for spheres and cylinders*, Proc. Roy. Soc. London Ser. A, 373 (1980), pp. 131–147.
[50] K. Stewartson and R. T. Waechter, *On Stefan's problem for spheres*, Proc. Roy. Soc. London Ser. A, 348 (1976), pp. 415–426.
[51] Y.-O. Tu, *A multi-phase Stefan problem describing the swelling and the dissolution of glassy polymer*, Quart. Appl. Math., 35 (1977), pp. 269–285.
[52] Y.-O. Tu and A. C. Ouano, *Model for the kinematics of polymer dissolution*, IBM J. Research Development, 21 (1977), pp. 131–142.
[53] B. Wu, S. W. McCue, P. Tillman, and J. M. Hill, *Single phase limit for melting nanoparticles*, Appl. Math. Model., 33 (2009), pp. 2349–2367.
[54] M. Hsieh, S. W. McCue, T. J. Moroney, and M. I. Nelson, *Drug diffusion from polymeric delivery devices: A problem with two moving boundaries*, in Proceedings of the 15th Biennial Computational Techniques and Applications Conference CTAC-2010, W. McLean and A. J. Roberts, eds., ANZIAM J. 52, Austral. Mathematical Soc., Australian National University, Canberra, Australia, 2011, pp. C549–C566.